RADIATION OF A MONOPOLE ANTENNA MOUNTED ON A CIRCULAR FLAT DISK

M. A. Hassan

Electrical Engineering Department
King Saud University
P. O. Box 800, Riyadh 11421
Saudi Arabia

الخلاصـــة :

نقدم في هذا البحث طريقة عزوم رقمية لحل مسألة الاشعاع الخاص بهوائي أحادي القطبية مركب عموديا عند مركز قرص دائري رفيع وموصل ومحدود الحجم . لقد طُبِّقت أولاً فكرة خطوط السريان الثابتة من أجل تمثيل القرص بمجموعة من الأسلاك ثم كوِّنت معادلات تكاملية للمجال الكهربائي من نوع (بوكلنجتن) لهوائي الأسلاك الناتج . وبعد ذلك تم حل هذه المعادلات بطريقة (بابنوف جالاركن) ذات المجال الكلي باستخدام كثيرات حدود (لاجرانج) كدوال أساسية . وقد استُخدِم ايضاً نموذج الثغرة محدودة العرض لتمثيل المنبع عند قاعدة الهوائي أحادي القطبية . وبمقارنة النتائج التي حصلنا عليها وجدناها تتفق ونتائج الطرق الأخرى السابق نشرها .

ABSTRACT

A numerical moment method is presented for solving the problem of radiation of a monopole antenna mounted perpendicularly on a perfect conducting finite circular thin disk at its center. The stationary lines of flow concept is first applied to simulate the disk with a wire grid model. Electric field integral equations of the Pocklington's type are then formulated for the resulting wire antenna structure. These, in turn, are solved by the entire domain Bubnov–Galerkin technique using Lagrangian interpolation polynomials as basis functions. A finite-width gap model is used to represent the source at the base of the monopole. The results obtained show good agreement with other methods available in the literature.

RADIATION OF A MONOPOLE ANTENNA MOUNTED ON A CIRCULAR FLAT DISK

1. INTRODUCTION

The behavior of dipole antennas in free space is well defined to all antenna engineers. A problem of continued interest is the behavior of such antennas when they are mounted on or placed near quite arbitrarily shaped conducting objects like aircraft, vehicles, ships, and buildings. The characteristics of interest, in these cases, include the radiation patterns, the input impedance and above all the currents induced on the surface of the conducting body.

The vertical monopole antenna above a circular ground horizontal plane is among those problems of practical importance. It is given special attention because it is commonly employed in airborne and ground-based communication systems at a wide range of frequencies. The electrical properties of such an antenna depend mainly on the size of the ground plane and the length and radius of the monopole. While the effect of an infinite plane can be easily predicted in terms of images, the effect of a plane of finite extent poses a much more difficult problem. The outer edge diffraction of the incident radiation modifies the currents on the ground plane and on the monopole from those of an infinite plane case. This diffraction becomes more and more significant as the ground plane size decreases.

Different techniques for dealing with the problem of a monopole above a circular conducting disk, have been used by different authors. Leitner and Spense [1] considered the case of a quarter-wavelength monopole above a circular disk of zero thickness, using the wave functions of the oblate spheroid and assuming a sinusoidal distribution of current on the antenna. Their method suffered from the serious restriction of using only a quarter-wavelength antenna, and their solution converged very slowly for the larger radii screens besides being of lengthy numerical computations. In an attempt to determine whether the disk was large enough to be considered as an infinite screen, and without putting any restriction on the length of the antenna, Storer [2, 3] used the variational method to solve the integral equation for the radial component of the electric field. He found that the effects of a finite screen decreased very slowly as the diameter of the screen increased. The input impedance was found [4] to uphold this conclusion as it approached the impedance of the infinite screen case for rather small values of the disk radius.

Thiele and Newman [5] combined the method of moments (MM) for the monopole with the geometrical theory of diffraction (GTD) for a disk larger or comparable to the wavelength. They used a magnetic frill representation—for the coaxial aperture at the base of the monopole—which closely modeled the actual physical geometry. They obtained agreement with experiment for both cases of the circular and the octagonal ground planes. However, as the number of sides of the octagonal disk increased, their method did not converge to the circular ground plane case. Also using GTD combined with MM, Awadalla and Maclean [6] extended the principle of the fictitious magnetic ring current, used for the circular ground plane, to the polygonal case, in order to obtain a good convergence to the circular shape as the number of sides of the polygon increased. The use of fictitious edge currents technique in the calculation of the input impedance was quite satisfactory, but, when it was applied to the radiation pattern, poor results were obtained, especially for smaller ground planes. Through the use of the equivalence theory, physically real estimated currents on the circular ground plane were obtained [7] and found to be useful in finding the radiation pattern, particularly for small ground planes.

Richmond suggested the sinusoidal–Galerkin moment method for a monopole at the center of a circular disk of radius not too large compared to the wavelength. He considered two cases. In the first case, the monopole–disk antenna was isolated in free space [8] and in the second it was placed over the flat earth [9]. Marin and Catedra [10] discussed the calculation of the input impedance of a monopole located at any point on a circular disk and oriented in an arbitrary direction using the combined techniques of GTD and MM with triangles and pulses as basis and testing functions. Weiner [11] compared the different input impedances and directive gains obtained by all the above methods for arbitrary antenna dimensions, and considered the best available results only.

Here in this paper, a technique different than those mentioned above is presented. The radiation problem of a monopole antenna placed vertically at the center of a perfect conducting finite circular thin disk is tackled, through the use of the method of moments [12], in order to find the current distribution on the antenna structure and hence calculate the far field pattern. The input impedance is also considered, mainly because besides being a quantity of interest in its own right, it is a good indicator of the overall accuracy in most moment method solutions. The stationary lines of flow concept is first applied and simulates the disk by thin radial wires interconnected at the center of the disk. Each of these wires and the monopole wire, is then represented by a single Pocklington's integral equation. The resulting set of integral equations is solved through the use of the entire domain Bubnov–Galerkin projective method. Lagrangian interpolation polynomial basis functions are used to approximate the currents on all wires. A finite-width gap model is used to represent the source at the base of the monopole. The results obtained show good agreement with the techniques mentioned above.

2. FORMULATION OF THE PROBLEM

2.1. Problem Configuration

Consider a monopole of length h located above a circular disk of radius R as shown in Figure 1. Both are made of perfect conductors and are infinitely thin; a is the radius of the wire and $2t$ is the disk thickness. The disk lies in the horizontal $x-y$ plane and the monopole is put vertically along the z-axis perpendicular to the disk with its lower end joining the disk at the center. The monopole is driven at the base, and $2g$ is the axial width of the gap across which a uniform field is impressed to represent the source of excitation. This width is very small in terms of wavelength.

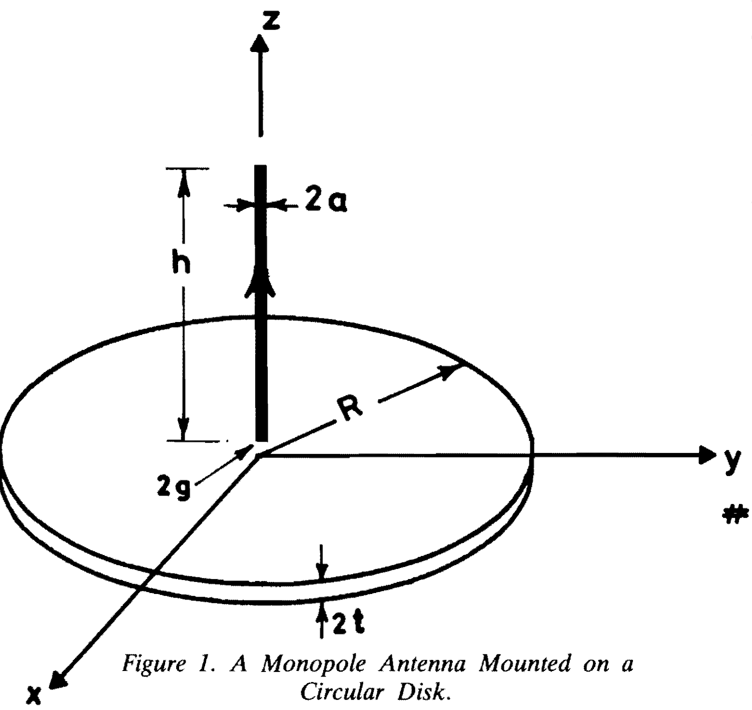

Figure 1. A Monopole Antenna Mounted on a Circular Disk.

2.2. Modeling the Disk by Radial Wires

The surface current $\mathbf{J}_s$ on a conducting surface induced by an electromagnetic field may be found by applying the boundary condition,

$$\mathbf{J}_s = \hat{\mathbf{n}} \times \mathbf{H} . \tag{1}$$

Equation (1) states that the current per unit width $\mathbf{J}_s$ over the surface of a perfect conductor is equal to the magnetic field strength $\mathbf{H}$ just outside the surface. The magnetic field and the surface current are parallel to the surface and perpendicular to each other; $\hat{\mathbf{n}}$ denotes a unit vector normal to the conductor.

For an isolated dipole along the z-axis in free space, the only existing magnetic field component is the azimuthal component H_ϕ. When a flat conducting plate is put horizontally near the dipole as shown in Figure 1, a surface current is induced. According to Equation (1), the directions of flow of this induced current are perpendicular to H_ϕ, *i.e.* along radial lines. If it is assumed that the surface current at any point can change in value but not in the path along which it flows, then such lines may be described as stationary lines of flow [13]. The orientation and distribution of the stationary lines of flow on the disk help the formation of its wire grid model. Therefore, the disk shown in Figure 1 may be modeled by a set of radial wires as shown in Figure 2. Their locations are directly related to the stationary lines of flow on the disk, and describe the path along which the

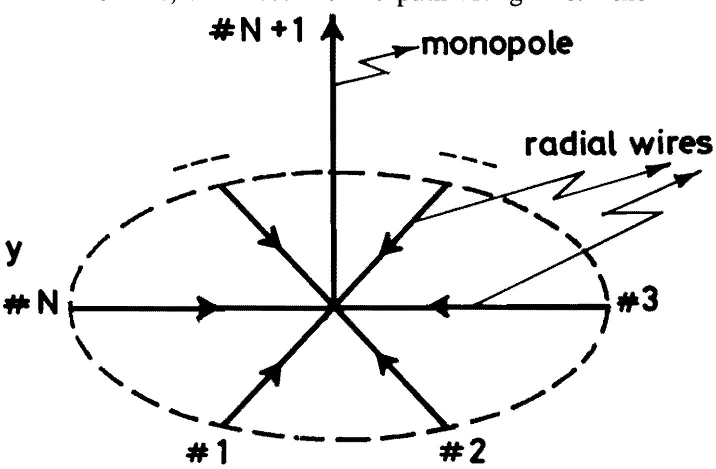

Figure 2. Modeling the Disk by N Radial Wires.

surface current flows. The arrows indicate the directions of current flow. The number of wires must be chosen to give as accurate results as possible. As more radial wires are added to simulate the ground disk, the more effective the screening of the monopole from the region below the disk becomes, and hence the closer the solution is to the exact one.

2.3. Electric Field Integral Equations

Consider that the disk is replaced by N radial thin wires, each having the same monopole radius a, as shown in Figure 2. The problem, in this case, is reduced to solving that of a wire antenna structure of $N+1$ wires interconnected at a single junction located at the center of the disk.

By applying the boundary condition requiring that the tangential electric field on the surface of each and every wire element is zero, $N+1$ electric field integral equations of the Pocklington's type can be formulated. Each of these wires, including the monopole, is represented by a single integral equation. Similar equations are obtained in a previous research work dealing with wire scatterers [14]. These equations are,

$$\frac{1}{\mathrm{j}\omega\varepsilon 4\pi} \sum_{m=1}^{N+1} \int_{0}^{l_m} I^m(s_m)\ F(s_n, s_m)\ \mathrm{d}s_m + \hat{\mathbf{n}} \cdot \mathbf{E}_n^{im}(s_n) = 0 \qquad n = 1,2,\ldots,N+1 \tag{2}$$

where $I^m(s_m)$ is the current at the source point s_m on wire element m whose length is l_m, and $F(s_n, s_m)$ is,

$$\begin{aligned} F(s_n, s_m) = {} & \frac{\exp(-\mathrm{j}\,k\,R_{mn})}{R_{mn}^5} \\ & \times [\hat{\mathbf{m}} \cdot \hat{\mathbf{n}}\, R_{mn}^2(-1-\mathrm{j}\,k\,R_{mn} + k^2\,R_{mn}^2) \\ & +(\mathbf{R}_{mn} \cdot \hat{\mathbf{m}})\,(\mathbf{R}_{mn} \cdot \hat{\mathbf{n}}) \\ & \times (3+\mathrm{j}\,3k\,R_{mn} - k^2\,R_{mn}^2)] \end{aligned} \tag{3}$$

R_{mn} is the distance between the field point s_n on wire n and the source point s_m on wire m. It is given by,

$$\begin{aligned} R_{mn}^2 = {} & (x_n - x_m + s_n\,\hat{\mathbf{x}} \cdot \hat{\mathbf{n}} - s_m\,\hat{\mathbf{x}} \cdot \hat{\mathbf{m}})^2 \\ & + (y_n - y_m + s_n\,\hat{\mathbf{y}} \cdot \hat{\mathbf{n}} - s_m\,\hat{\mathbf{y}} \cdot \hat{\mathbf{m}})^2 \\ & + (z_n - z_m + s_n\,\hat{\mathbf{z}} \cdot \hat{\mathbf{n}} - s_m\,\hat{\mathbf{z}} \cdot \hat{\mathbf{m}})^2 + a_n^2 \end{aligned} \tag{4}$$

(x_n, y_n, z_n) and (x_m, y_m, z_m) are the cartesian coordinates of one end of wire elements n and m respectively. $\hat{\mathbf{m}}$ and $\hat{\mathbf{n}}$ are unit vectors along the wires m and n respectively, and show the direction of current flow along the wire. k is equal to 2π/wavelength. $\mathbf{E}_n^{im}(s_n)$ is the tangential component of the impressed electric field along wire n at point s_n. Simple harmonic time dependence at angular frequency ω, $\exp(\mathrm{j}\omega t)$, is assumed and will be suppressed in all field quantities. ε is the permittivity of the medium.

3. BUBNOV–GALERKIN SOLUTION

3.1. Generation of the Matrix Equation

The solution of the system of integral equations are obtained through the use of the entire domain Bubnov–Galerkin projective method with Lagrangian interpolation functions used as basis functions [14]. Therefore, the current in (2) is first approximated by,

$$I^m(s_m) = \sum_{p=1}^{L} I_p^m\ \phi_p(s_m) \tag{5}$$

where ϕ is the interpolation polynomial,

$$\phi_p(s_m) = \frac{(s_m - s_1)\ldots(s_m - s_{p-1})\,(s_m - s_{p+1})\ldots(s_m - s_L)}{(s_p - s_1)\ldots(s_p - s_{p-1})\,(s_p - s_{p+1})\ldots(s_p - s_L)}$$

and the node s_p is given by

$$s_p = (p-1)\,l_m/(L-1)\ , \quad p = 1,2,\ldots,L\ ,$$

L is the number of interpolation nodes along the wire, and $(I_p^{m}, p = 1,\ldots,L)$ are the unknown complex current coefficients to be determined.

Taking the inner product projection of both sides of (2) onto the subspace spanned by the basis functions, the following set of linear algebraic equations are obtained,

$$\begin{aligned} & \frac{\mathrm{j}\,\eta}{4\pi\,k} \sum_{m=1}^{N+1} \sum_{p=1}^{L} \\ & \times I_p^m \left\{ \int_{0}^{l_n} \phi_i(s_n) \int_{0}^{l_m} \phi_p(s_m)\ F(s_n, s_m)\ \mathrm{d}s_m\ \mathrm{d}s_n \right\} \\ & = \int_{0}^{l_n} \hat{\mathbf{n}} \cdot \mathbf{E}_n^{im}(s_n)\ \phi_i(s_n)\ \mathrm{d}s_n \\ & i = 1,2,\ldots,L\ , \quad n = 1,2,\ldots,N+1\ , \end{aligned} \tag{6}$$

where η is the intrinsic impedance of the medium. The impedance matrix elements of the left hand side of (6), contain near singular integrand of either of two types. Diagonal elements, generated when the source and field points are on the same wire and approach each other (*i.e.* $s_m \simeq s_n$), involve a singularity of the type encountered before [15]. However, off-diagonal elements, obtained when the source and field points are on two different wires and approach the junction point (*i.e.* $s_m \simeq s_n \simeq 0$), also contain near singular integrands. These are of two different forms depending on whether the two wires are collinear or are forming an angle between them. The latter two cases are previously encountered and treated in earlier research works [14, 16]. At the junction of all wires at the center of the disk, Kirchhoff's current law is applied resulting in an equation which reduces the number of unknowns of (6) by one. The appendix shows how this is enforced during computations.

3.2. Determination of the Excitation Vector

The present problem is on radiation of the monopole mounted on a circular disk. The source of excitation is at the base of the monopole. It can be modeled as a dielectric gap across which a time harmonic excitation voltage $V \exp(j\omega t)$ is maintained, V being the complex voltage amplitude, and ω the radian frequency. The base-fed monopole represents the physical model for the field source on the antenna structure under consideration. Mathematically, this could be represented by the delta-gap model in which the voltage V is maintained across an infinitesimal gap. Despite the immense success of his model in the far field computations, the delta generator has been criticized on many occasions, mainly on physical grounds. An alternative model is the magnetic frill which appears to be a nearer approximation to the actual source, as in the case of an infinite plane structure. The ground plane considered here, is assumed to be of finite electrical dimension. Hence, the finite-width gap model is thought to be, more suitable to the present application. Also, it was found to be an adequate model for the source for far field pattern and current distribution computations on straight wire antennas [15]. The boundary conditions on the impressed field across the finite-width gap, shown in Figure 1, can be stated in the form,

$$E_n^{im} = \left\{ \begin{array}{ll} \dfrac{V}{g} & 0 \leqslant s_n \leqslant 2g \\ 0 & \text{elsewhere on the monopole} \end{array} \right\} \qquad (7)$$

By substituting (7) in the R.H.S. of Equation (6), the excitation vector will be a string of zeroes except at the entry corresponding to the first node, of the monopole, at which the source is located, as in Equation (8).

$$\text{R.H.S.} = \begin{bmatrix} 0 \\ 0 \\ \vdots \\ 1 \\ 0 \\ 0 \end{bmatrix} \begin{array}{l} \\ \\ \\ \leftarrow \text{corresponds to the first node} \\ \quad \text{at the base of the monopole} \\ \\ \end{array} \qquad (8)$$

Here, the excitation voltage has been normalized to 1 volt.

4. RADIATION FIELD FOR THIN WIRES

Once the current coefficients are obtained from the solution of (6), the far field pattern can be easily determined. The radiation field at any point in space is given by the vector sum of the fields of all wire currents.

Consider one of the wires modeling the disk, as shown in Figure 3. Its ends are labeled with (x_1, y_1, z_1) and (x_2, y_2, z_2). The magnetic vector potential, at point $f(r, \theta, \phi)$, expressed in terms of the spherical coordinates, is,

$$\mathbf{A} = \hat{\mathbf{m}} \int_0^{l_m} I_m(s_m)\, \mu\, \frac{\exp(-j\,k\,R_{mf})}{4\pi R_{mf}}\, ds_m \qquad (9)$$

where μ is the permeability of the medium, and

$$\hat{\mathbf{m}} = \hat{\mathbf{x}}\left(\frac{x_1 - x_2}{l_m}\right) + \hat{\mathbf{y}}\left(\frac{y_1 - y_2}{l_m}\right) + \hat{\mathbf{z}}\left(\frac{z_1 - z_2}{l_m}\right) \qquad (10)$$

and

$$\begin{aligned} R_{mf}^2 = {} & \{r \sin\theta \cos\phi - (x_2 + s_m\, \hat{\mathbf{x}} \cdot \hat{\mathbf{m}})\}^2 \\ & + \{r \sin\theta \sin\phi - (y_2 + s_m\, \hat{\mathbf{y}} \cdot \hat{\mathbf{m}})\}^2 \\ & + \{r \cos\theta - (z_2 + s_m\, \hat{\mathbf{z}} \cdot \hat{\mathbf{m}})\}^2 \,. \end{aligned} \qquad (11)$$

For large values of r, Equation (11) reduces to

$$\begin{aligned} R_{mf} = {} & [\mathrm{r} - \sin\theta \cos\phi (x_2 + s_m\, \hat{\mathbf{x}} \cdot \hat{\mathbf{m}}) - \sin\theta \sin\phi \\ & \cdot (y_2 + s_m\, \hat{\mathbf{y}} \cdot \hat{\mathbf{m}}) - \cos\theta (z_2 + s_m\, \hat{\mathbf{z}} \cdot \hat{\mathbf{m}})] \,. \end{aligned} \qquad (12)$$

At the far field point, the electric field components are:

$$\left. \begin{aligned} E_\theta &= -j\,\omega\, \mathbf{A} \cdot \hat{\boldsymbol{\theta}} \\ E_\phi &= -j\,\omega\, \mathbf{A} \cdot \hat{\boldsymbol{\phi}} \,, \end{aligned} \right\} \qquad (13)$$

where the spherical unit vectors $\hat{\boldsymbol{\theta}}$ and $\hat{\boldsymbol{\phi}}$ may be expressed in terms of the cartesian unit vectors as,

$$\left. \begin{aligned} \hat{\boldsymbol{\theta}} &= \hat{\mathbf{x}} \cos\phi \cos\theta + \hat{\mathbf{y}} \sin\phi \cos\theta - \hat{\mathbf{z}} \sin\theta \\ \hat{\boldsymbol{\phi}} &= -\hat{\mathbf{x}} \sin\phi + \hat{\mathbf{y}} \cos\phi \end{aligned} \right\} \qquad (14)$$

Substituting (9) and (14) into (13), considering m and R_{mf} of (10) and (12) respectively, and also considering the $N+1$ wires of Figure 2, we obtain

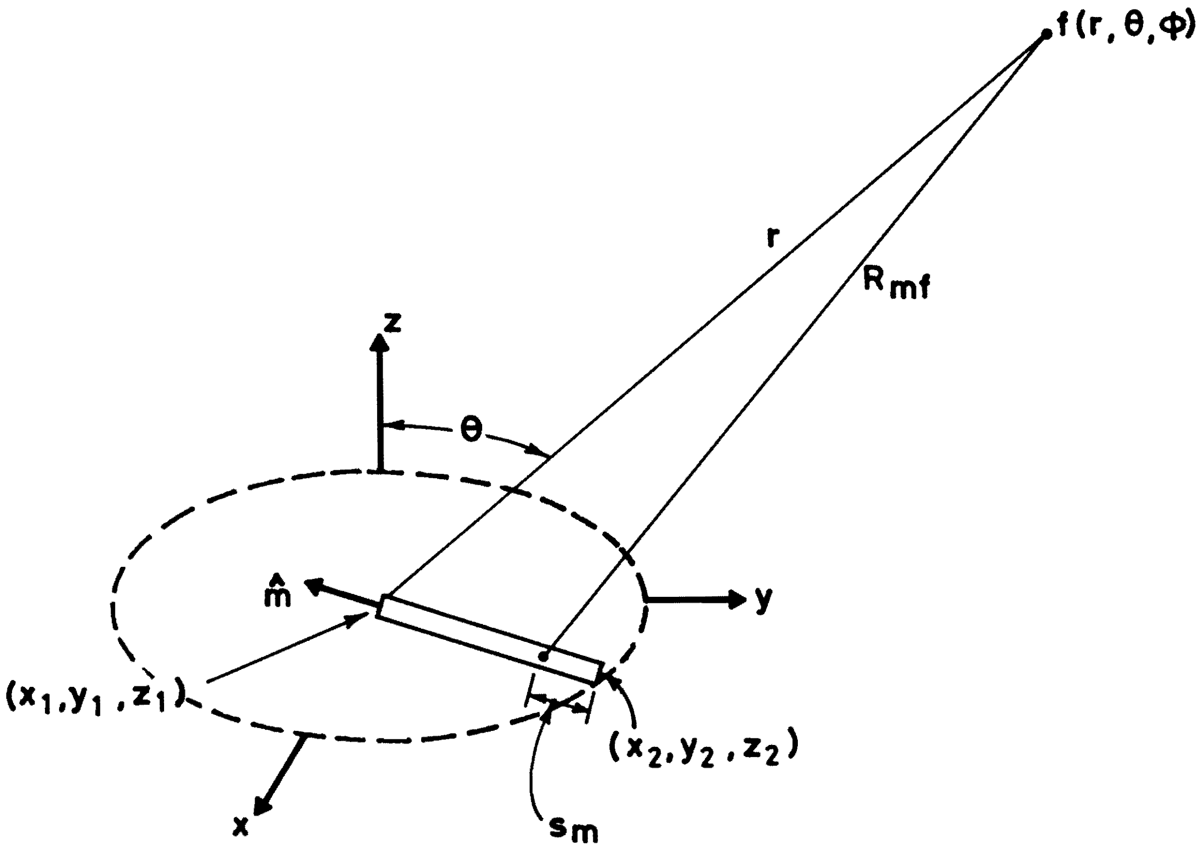

Figure 3. Calculation of the Radiation Field of a Wire.

$$E_\theta(r,\theta,\phi) = -\mathrm{j}\,\omega\,\mu\,\frac{\exp(-\mathrm{j}\,k\,r)}{4\pi\,r}\sum_{m=1}^{N+1}\int_0^{l_m} I_m(s_m)$$
$$\cdot \exp(\mathrm{j}\,k\,q)\,\mathrm{d}s_m \cdot [(\hat{\mathbf{x}}\cdot\hat{\mathbf{m}})\cos\phi\cos\theta$$
$$+(\hat{\mathbf{y}}\cdot\hat{\mathbf{m}})\sin\phi\cos\theta-(\hat{\mathbf{z}}\cdot\hat{\mathbf{m}})\sin\theta] \tag{15a}$$

$$E_\phi(r,\theta,\phi) = -\mathrm{j}\,\omega\,\mu\,\frac{\exp(-\mathrm{j}\,k\,r)}{4\pi\,r}\sum_{m=1}^{N+1}\int_0^{l_m} I_m(s_m)$$
$$\cdot \exp(\mathrm{j}\,k\,q)\,\mathrm{d}s_m \cdot [-(\hat{\mathbf{x}}\cdot\hat{\mathbf{m}})\sin\phi$$
$$+(\hat{\mathbf{y}}\cdot\hat{\mathbf{m}})\cos\phi] \tag{15b}$$

where $q = \sin\theta\cos\phi(x_2+s_m\,\hat{\mathbf{x}}\cdot\hat{\mathbf{m}})+\sin\theta\sin\phi$
$\cdot(y_2+s_m\,\hat{\mathbf{y}}\cdot\hat{\mathbf{m}})+\cos\theta(z_2+s_m\,\hat{\mathbf{z}}\cdot\hat{\mathbf{m}})$

The integration appearing in (15) is easily evaluated using a simple Gauss–Legendre quadrature formula.

5. NUMERICAL RESULTS

In this section, numerical results are given in order to illustrate the ability of the present approach in the analysis of a monopole above a circular finite disk. Based on the above equations, a digital computer program, written in FORTRAN and run on the digital equipment corporation VAX 11/785 computer, is developed. The problem under consideration is solved here for the current distribution, input impedance and far field pattern and for different disk radii so as to allow the comparison with Richmond and Awadalla's results. A normalized voltage source of 1 volt is taken to be at the base of the monopole. The disk is modeled once with 8 wires and a second time with 16 wires. Their radii are taken to be the same as the monopole radius. The current on the monopole is approximated by a second order polynomial while it is approximated on those wires modeling the disk by second, third, and fourth order polynomials when $0.2\,\lambda \leq R \leq 0.5\,\lambda$, $0.5\,\lambda \leq R \leq 1.0\,\lambda$, and $1.0\,\lambda \leq R \leq 1.4\,\lambda$ respectively.

The thin circular metallic disk with the monopole at the center is solved for different values of the disk radius R ranging between 0.2λ and 1.4λ. The monopole length and radius are respectively 0.229λ and 0.003λ. By modeling the disk by 8 radial wires, the input impedance of the antenna is computed, plotted in Figure 4, and compared with that obtained by Richmond [8]. It is clear that they agree well for smaller disk sizes and diverge a little for larger sizes. For more comparisons, another problem is considered here and compared with another technique, namely that of Awadalla and Maclean [6]. The input impedance of a $\lambda/4$ monopole of diameter ⅛ inch on a circular disk of diameter 3 feet is computed and illustrated in Figure 5. Close agreement is shown between both results for both the resistance and reactance components of the input impedance. In this case, the disk is also modeled by 8 radial wires.

When the monopole length is changed to 0.25λ keeping its radius at 0.003λ, the current distributions on the radial wires of the circular disk are computed and plotted in Figure 6 for different disk radii. This has been considered for the two wire models of the disk. No fundamental difference was shown between both cases. Although the currents at the free ends of the wires are not forced to be zero, yet the current distributions show fairly good zeros at those ends. Richmond's results [8] could also be well compared with our results, however, they are not shown here for the sake of clarity. It is worthwhile to note that the increase of the number of wires—modeling the disk—will, of course, improve the computed current distribution. However, this will be at the expense of an increase in the computational time and effort, without gaining much accuracy in the far field pattern and input impedance. Therefore, the upper limit on the number of wires is decided by answering the following question; "How much accurate the result is needed and how much computational time and effort are afforded to spend to reach such accuracy?" On the other hand, there is always a minimum number of wires below which the wire grid model is said to be "incorrect", *i.e.* giving inaccurate results. This, mainly, depends on the monopole and disk dimensions.

Also, illustrated in Figure 7, is the far field pattern (E_θ *versus* θ) for a monopole of length 0.25λ and radius 0.0026λ on a circular disk of radius 0.6λ. The disk is modeled by 16 radial wires. Also shown for comparison are the results obtained by Awadalla and Maclean [7].

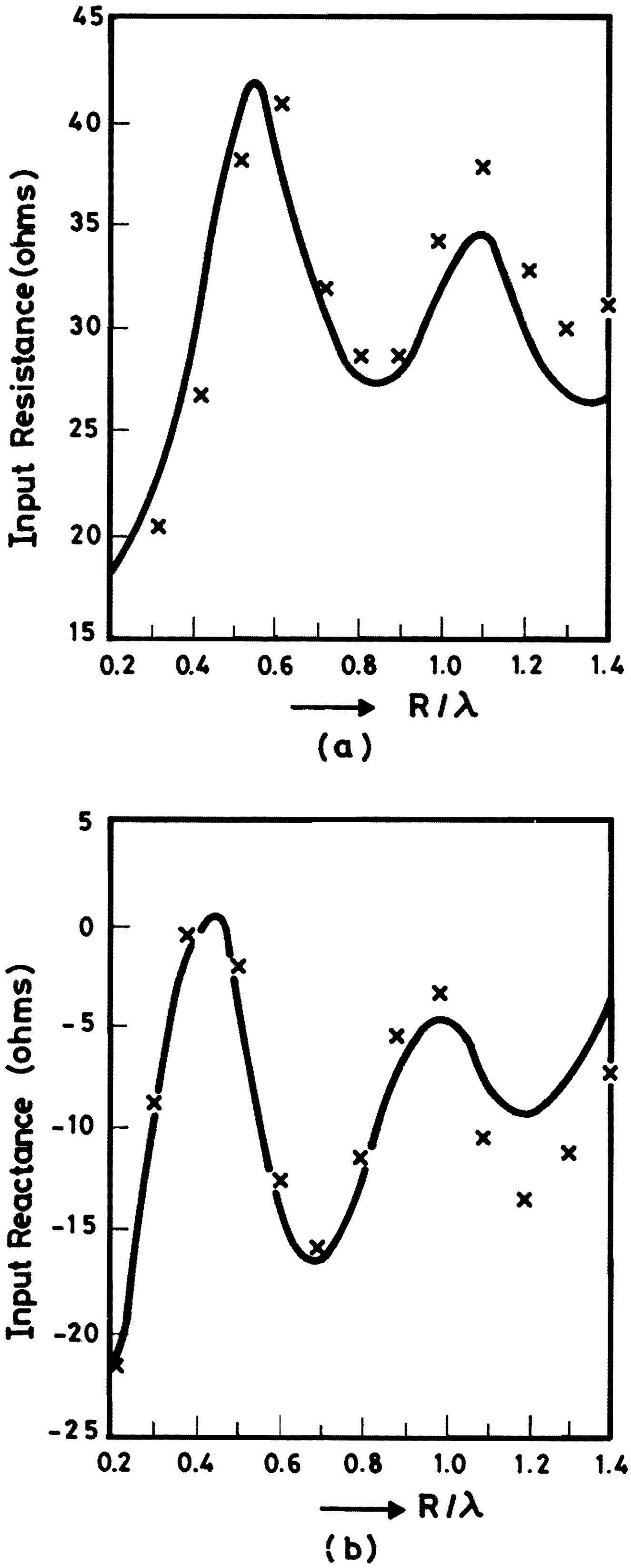

Figure 4. Input Impedance of a Monopole (h = *0.229* λ, a = *0.003* λ) *as a Function of the Disk Radius* R. ___ This Method; × × × Richmond [8].

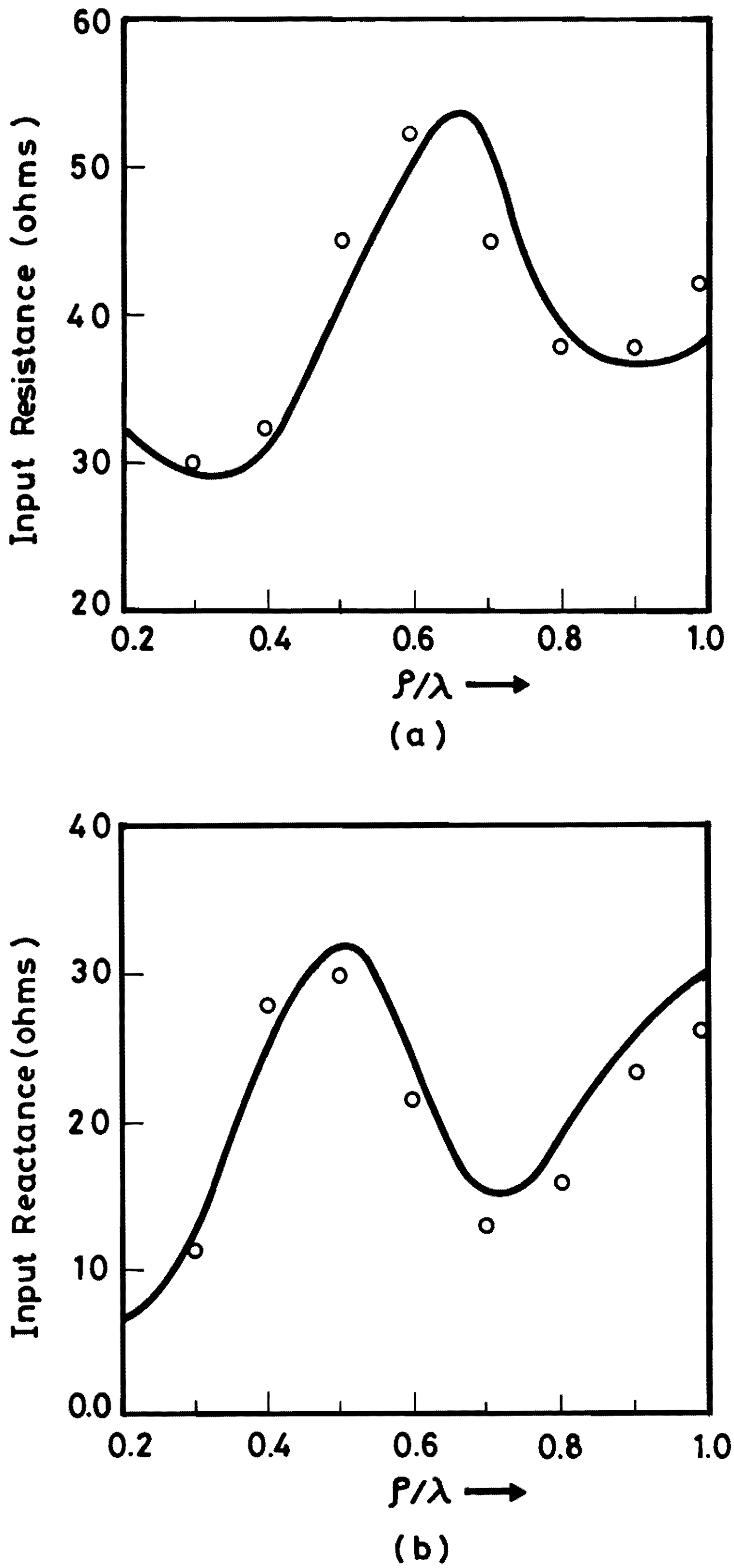

Figure 5. Input Impedance of a Monopole (h = 0.25 λ, a = 0.0625 in) on a Circular Disk of Diameter 3 feet. —— This Method; ○○○ Awadalla and Maclean [6].

6. CONCLUSION

The surface current, input impedance, and radiation pattern are obtained for a monopole antenna radiating in the presence of and mounted on a perfect conducting circular thin disk. The disk is first modeled by radial wires using the stationary lines of flow concept. Then, the solution of the resulting wire structure is obtained through the use of an entire domain Galerkin's formulation. Radial wires are found to act essentially the same as the continuous metallic disk surface which they replace without significant alteration to the results. Discrepancies shown in the comparison, may be due to insufficient number of wires modeling the disk resulting in a bad screening for the monopole, or due to considering those wire radii equal to the monopole radius. Good results are obtained for disks with radii about one wavelength or less. For larger radii, the accuracy drops off rapidly due to the finite number of quadrature nodes used in performing the integrations of the matrix elements. Also the solution diverges when more than fourth or fifth order polynomials are used. Computation is greatly reduced because of the symmetry of the problem and its chosen model. Typical CPU time on VAX 11/785 is around 2 minutes for an 8-wire disk model and 10 minutes for a 16-wire disk model when second order polynomials are used on all wires. This is about 10 times (or over) slower than corresponding runs on the IBM 3083

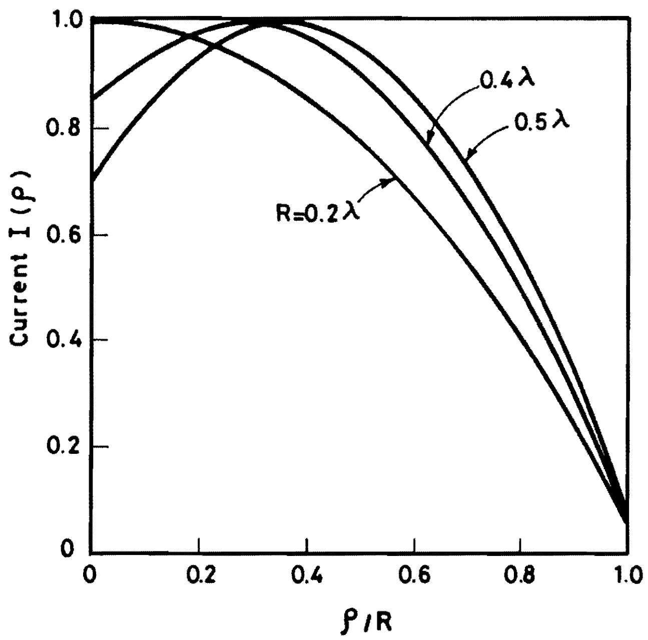

Figure 6. Current Distribution on the Radial Wires of the Circular Disk of Figure 2. Monopole Length = 0.25 λ and Monopole Radius = 0.003 λ for Different Disk Radii.

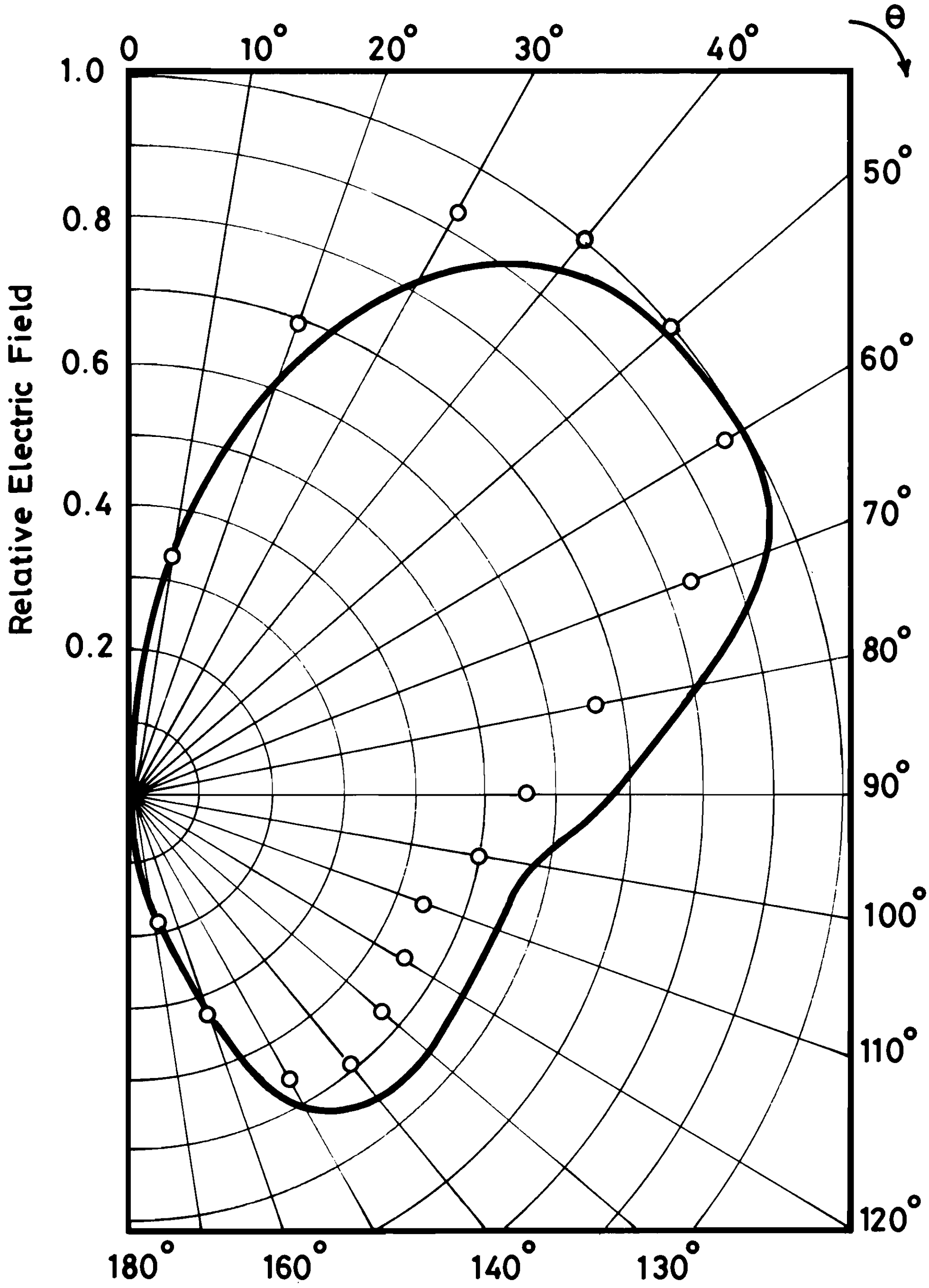

Figure 7. Radiation Pattern ($E_\theta \rightarrow \theta$) of a Monopole on a Circular Disk of Radius 0.6 λ. Monopole Length = 0.25 λ, Monopole Radius = 0.0026 λ. —— This Approach; ○○○ Awadalla and Maclean [7].

computer. Comparisons of the results with previous computations show good agreement in general.

REFERENCES

[1] A. Leitner and R. D. Spence, "Effect of a Circular Ground Plane on Antenna Radiation", *Journal of Applied Physics,* **21** (1950), p. 1001.

[2] J. E. Storer, "The Impedance of an Antenna Over a Large Circular Screen", *Journal of Applied Physics,* **22** (1951), p. 1058.

[3] J. E. Storer, "The Radiation Pattern of an Antenna Over a Circular Ground Screen", *Journal of Applied Physics,* **23** (1952), p. 588.

[4] R. F. Hahn and J. G. Fikioris, "Impedance and Radiation Pattern of Antennas Above Flat Discs",

IEEE Transactions on Antennas and Propagation, **21** (1973), p. 97.

[5] G. A. Thiele and T. H. Newhouse, "A Hybrid Technique for Combining Moment Methods with the Geometrical Theory of Diffraction", *IEEE Transactions on Antennas and Propagation,* **23** (1975), p. 62.

[6] K. H. Awadalla and T. S. M. Maclean, "Input Impedance of a Monopole Antenna at the Center of a Finite Ground Plane", *IEEE Transactions on Antennas and Propagation,* **26** (1978), p. 244.

[7] K. H. Awadalla and T. S. M. Maclean, "Monopole Antenna at Center of Circular Ground Plane: Input Impedance and Radiation Pattern", *IEEE Transactions on Antennas and Propagation,* **27** (1979), p. 151.

[8] J. H. Richmond, "Monopole Antenna on Circular Disk", *IEEE Transactions on Antennas and Propagation,* **32** (1984), p. 1282.

[9] J. H. Richmond, "Monopole Antenna on Circular Disk Over Flat Earth", *IEEE Transactions on Antennas and Propagation,* **33** (1985), p. 633.

[10] M. Marin and M. F. Catedra, "A Study of a Monopole Arbitrarily Located on a Disk Using Hybrid MM/GTD Techniques", *IEEE Transactions on Antennas and Propagation,* **35** (1987), p. 287.

[11] M. M. Weiner, "Monopole Element at the Center of a Circular Ground Plane Whose Radius is Small or Comparable to a Wavelength", *IEEE Transactions on Antennas and Propagation,* **35** (1987), p. 488.

[12] R. F. Harrington, *Field Computation by Moment Methods.* New York: Macmillan, 1968.

[13] J. Aharoni, *Antennae: An Introduction to Their Theory.* Oxford: Clarendon Press, 1946.

[14] M. A. Hassan, P. Silvester, B. Howarth, and N. Nasu, "Solution to the Interconnected Wire Scatterer Problem", *Proceedings of the Institution of Electrical Engineers,* **123** (1976), p. 509.

[15] P. Silvester and K. K. Chan, "Analysis of Antenna Structures Assembled from Arbitrarily Located Straight Wires", *Proceedings of the Institution of Electrical Engineers,* **120** (1973), p. 21.

[16] M. A. Hassan, "Solution of a Monopole Antenna Over a Circular Finite Disk", *Proceedings of the International IEEE/APS Symposium, Philadelphia, Pennsylvania,* 1986, p. 133.

Paper Received 4 April 1988; Revised 9 July 1989.

APPENDIX

At the junction (*i.e.* at the center of the disk), Kirchhoff's current law must be satisfied. Consider the $N+1$ wire structure shown in Figure A, and let the current on each wire be represented by a quadratic polynomial (*i.e.* three interpolation nodes on each wire). Apply Kirchhoff's current law at the junction,

$$I_3 + I_6 + I_9 + \ldots I_{3N} = I_{3N+1} \qquad \text{(A.1)}$$

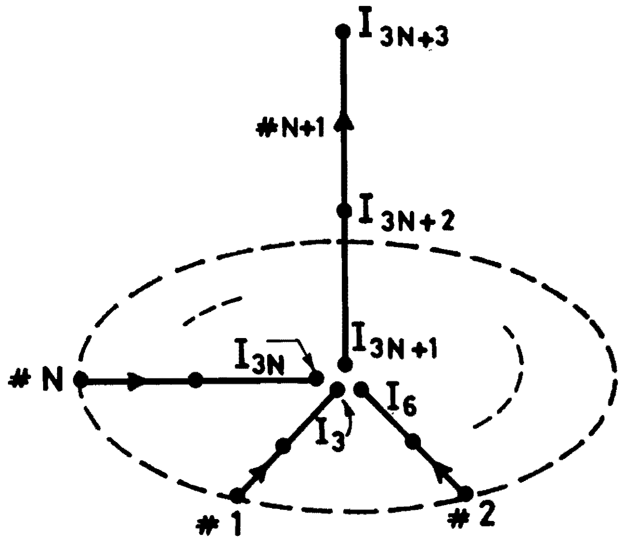

Figure A. Junction of N+1 *Nodes at the Center of the Disk.*

Equation (A.1) will reduce the number of unknowns ($3N+3$) by one. The relation between the interpolation coefficients of the conjoint structure and that of the corresponding disjoint structure can be obtained if we consider (A.1) as a mapping of the ($3N+2$) unknowns of the conjoint structure into the ($3N+3$) unknowns of the disjoint structure [15] (Equation (A.2)).

$$\begin{bmatrix} I_1 \\ I_2 \\ I_3 \\ : \\ : \\ I_{3N} \\ I_{3N+1} \\ I_{3N+2} \\ I_{3N+3} \end{bmatrix} = \begin{bmatrix} 1 & & & & & & & \\ & 1 & & & & & & \\ & & 1 & & & & & \\ & & & \ddots & & & & \\ & & & & \ddots & & & \\ & & & & & 1 & & \\ 0 & 0 & 1001 & \ldots & & 1 & 0 & 0 \\ & & & & & & 1 & 0 \\ & & & & & & & 1 \end{bmatrix} \begin{bmatrix} I_1 \\ I_2 \\ I_3 \\ : \\ : \\ I_{3N} \\ I_{3N+2} \\ I_{3N+3} \end{bmatrix} \qquad \text{(A.2)}$$

Equation (A.2) may be written in matrix form as

$$I^{\mathrm{dis}} = C\, I^{\mathrm{con}} . \qquad \text{(A.3)}$$

Substitution of (A.3) into

$$Z^{\mathrm{dis}}\, I^{\mathrm{dis}} = V^{\mathrm{dis}} , \qquad \text{(A.4)}$$

(corresponding to Equation (6) of the disjoint structure) and premultiplication by C^{T} yields

$$C^{\mathrm{T}}\, Z^{\mathrm{dis}}\, C\, I^{\mathrm{con}} = C^{\mathrm{T}}\, V^{\mathrm{dis}} \qquad \text{(A.5)}$$

which can be put in the form

$$Z^{\mathrm{con}} I^{\mathrm{con}} = V^{\mathrm{con}} \tag{A.6}$$

where,

$$Z^{\mathrm{con}} = C^{\mathrm{T}} Z^{\mathrm{dis}} C \tag{A.7}$$

and

$$V^{\mathrm{con}} = C^{\mathrm{T}} V^{\mathrm{dis}} . \tag{A.8}$$

Evaluation of (A.7) requires simple row and column operations on the existing coefficient matrix Z^{dis}, while to evaluate (A.8), only row operations are required on the excitation vector V^{dis}. Equation (A.6) is then solved for the unknown current coefficients I^{con}.